Multi-dimensional Ablation and Thermal Response Program for Martian Entry Analysis

Viola Renato[1] and Thomas Scanlon[1]

[1] *Aerospace Centre of Excellence, University of Strathclyde, Glasgow, Scotland, United Kingdom*

Abstract

A new method to simulate ablative Thermal Protection System (TPS) behaviour during an atmospheric entry is presented. The approach consists of the coupling of two reduced order codes: one for the material behaviour prediction and one for the external heat flux estimation. The latter is a reduced order aero-thermodynamic code developed at Strathclyde University while the internal solver is a unidimensional thermo-ablative code. The three-dimensional spacecraft calculations are generated by running the one-dimensional ablative code on every geometrical vertex. This method produces an estimation of the 3D problem solution while avoiding the complexity of a multidimensional thermo-ablative solver. The test case analysed to prove the method efficacy is the entry of the Pathfinder capsule in the Martian atmosphere.

Keywords: Ablation, Thermal Protection, Modelling, Re-Entry

Nomenclature

A	:	pre-exponential constant, s^{-1}
B'	:	dimensionless mass blowing rate
C_H	:	Stanton number for heat transfer
C_M	:	Stanton number for mass transfer
c_p	:	specific heat, $J/kg\text{-}K$
E	:	activation temperature, K
F	:	view factor
h	:	enthalpy, J/kg
$\overline{h}$	:	partial heat of charring, J/K
$\dot{m}_g$	:	pyrolysis gas mass flux, $kg/m^2 s$
q_{rad}	:	radiative heat flux, W/m^2
q_{cond}	:	conductive heat flux, W/m^2
$\dot{S}$	:	surface recession rate, m/s
T	:	temperature, K
t	:	time, s
u	:	velocity, m/s
x	:	space coordinate, m
α_w	:	surface absorption
ϵ	:	surface emissivity
k	:	thermal conductivity, W /m-K
ρ	:	density, kg/m^3
σ	:	Stefan-Boltzman constant, $W/m^2\text{-}K^4$
τ	:	virgin mass fraction
ψ	:	decomposition reaction order

Subscripts

c	:	charred
e	:	boundary layer edge
g	:	pyrolysis gas
i	:	i component
v	:	virgin
w	:	wall

Introduction

In space missions, the atmospheric entry phase presents a critical challenge for the spacecraft design due to the extreme external temperatures that the spacecraft must endure. Thermal protection systems (TPS) are required to prevent any damage to the spacecraft, its internal components or passengers. TPS are generally divided into two major categories: reusable and non-reusable. Ablative materials are part of the latter group and they are very common and highly reliable. These materials perform their task through the pyrolysis phenomenon: an endothermic process that consumes external thermal energy to generate a change of state in the material itself, leading to material degradation. This process is complex and not trivial to simulate. Nevertheless, a considerable number of ablative material behaviour prediction tools exist and these tools are widely applied in space research and industry. One of the most accurate ways to perform thermal protection analyses is to consider both the internal and external thermal energy balances and examine how the two interact with each other. The external analysis is generally performed by a CFD solver which can produce highly precise results however it can be computationally demanding. In the present approach the aerodynamics simulations are performed by a reduced order code, Hyflow [1].

The material behaviour predictions are generated by another in-house code. The selected test case is the entry of the Mars Pathfinder into the Martian atmosphere. It was chosen for two main reasons: to demonstrate the ability of the current approach to

simulate a passage in an atmosphere different from Earth's and because Mars is currently a very important topic in the space field. There are many Martian missions in various design phases, manned and unmanned, and the ability to simulate an approximated but close to reality, three dimensional behaviour of the TPS in a Mars entry could give a significant advantage in the selection of the most efficient TPS solutions for any of those missions. Analyses on similar test cases and on the exact mission studied in this paper are present in the literature; the majority of these evaluations are carried out employing codes that can perform very accurate two or three dimensional ablative simulations; in addition, they are often coupled with CFD solvers which evaluate the external environmental conditions during the entry.

The adoption of highly accurate tools improves the precision of the studies but also increases the computational resources required, which can be counter productive in the preliminary phases of a mission design when it is necessary to preform a great variety of calculations in order to evaluate the best solution to meet the mission requirements. Olynick et al [2] used the flow solver GIANTS for the air prediction and FIAT for the material behaviour estimation; the same codes were employed by Milos et al [3] for part of the Pathfinder analyses presented in their paper. Martin and Boyd [4] presented results generated with LeMANS (Unstructured Tridimensional Navier Stokes Solver for Hypersonic Nonequilibrium Aerothermodynamics) and MOPAR as the material response code.

Material Response code

Degradation process

The pyrolysis phenomenon is manifested through a change of state in the material during which its density decreases and the material undergoes a degradation[5]. The code employed in this paper presents a three components degradation model to better imitate the real behaviour of the ablative material. The material density is calculated using Eq. 1, where the subscripts A and B refer to the resin filler components, the letter C refers to the reinforcing material and Γ is the volume fraction of the resin.

$$\rho = \Gamma(\rho_A + \rho_B) + (1 - \Gamma)\rho_C. \tag{1}$$

The pyrolysis process is described by an Arrhenius equation for each component:

$$\frac{\partial \rho_i}{\partial t} = A_i \left(\frac{\rho_i - \rho_{ic}}{\rho_{iv} - \rho_{ic}} \right)^{\phi_i} e^{-E_i/T}. \tag{2}$$

where A_i, E_i, ϕ_i, ρ_{iv}, ρ_{ic} are respectively the pre-exponential factor, activation energy, decomposition reaction order, virgin and charred density for the component i=A,B,C. The terms in Eq. 2 are empirically estimated using thermal gravimetric analysis (TGA)[6].

In-depth energy equation

The following equation describes the internal exchanges of energy in the TPS thickness,

$$\rho c_p \frac{\partial T}{\partial t} = \frac{\partial}{\partial x}\left(k \frac{\partial T}{\partial x} \right) + (h_g - \overline{h}) \frac{\partial \rho}{\partial t} + \dot{S} \rho c_p \frac{\partial T}{\partial x} + \dot{m}_g \frac{\partial h_g}{\partial x} \tag{3}$$

the terms forming Eq.3 can be interpreted as: rate of storage of sensible energy, net rate of thermal conduction, pyrolysis energy rate, convection rate of sensible energy due to coordinate system movement, and net rate of energy convected with pyrolysis gas passing a point. The thermal conduction and the pyrolysis energy rate are the only terms which are implemented in this approach, the other two terms in Eq. 3 are neglected in order to decrease the computational time required to complete the simulations. This procedure introduces some errors in the estimated results, however these errors do not appear to greatly decrease the result accuracy as it will be shown in the results section.

The local specific heat is a function of both virgin and charred specific heat values and the local charring state; it is formulated as shown in Eq. 4.

$$c_p = \tau c_{pv} + (1 - \tau) c_{pc}. \tag{4}$$

where τ represents the virgin mass fraction. The thermal conductivity k is evaluated by applying the equivalent equation.

Boundary conditions

The external surface energy balance is calculated using the equation:

$$\rho_e u_e C_H (H_r - h_w) + \rho_e u_e C_M [\Sigma (z^*_{ie} - z^*_{iw}) h_i^{T_w} - B' h_w] + \dot{m}_c h_c + \dot{m}_g h_g + \alpha_w q_{rad} - F \sigma \epsilon_w T_w^4 - q_{cond} = 0. \tag{5}$$

The individual terms in Eq. 5 represent: convective flux, chemical energy rate, rate of radiant energy input to the ablating in surface, rate of radiant energy emission from the ablating out surface and rate of energy conduction into the ablating material. In the proposed approach the chemical energy rate terms are neglected. As in the case of Eq. 3,this introduces

some errors and decreases the precision of the generated results; nevertheless the result accuracy is high enough to give a good understanding of all the phenomena involved and their roles influencing the material responses, as it will be illustrated in the next sections when the calculations produced by the presented approach are compared against validated code results.

Pyrolysis gas and Char production

During the degradation, the material decreases its density and produces pyrolysis gases. The assumption utilized in this approach is that the whole mass equivalent to density decrease is transformed into pyrolysis gases and that all the produced gas exits the material each time step. Following these assumptions the mass flow rate of the pyrolysis gas can be evaluated as follows [7]:

$$\dot{m}_g = \frac{1}{A}\int_{x_0}^{x_w}\left(\frac{\partial\rho}{\partial t}\right)A\partial x. \tag{6}$$

Blowing correction

The blocking effect due to the exiting of the pyrolysis gas is introduced through the correction of the heat transfer, C_H according to the equation[5]:

$$\frac{C_H}{C_{H0}} = \frac{\zeta}{e^{\zeta}-1} \tag{7}$$

$$\zeta = \frac{2\lambda(m_g+m_c)}{\rho U_e C_{H0}} \tag{8}$$

where λ is equal to 0.5 in the classical blowing correction formula [5].

Aero-Thermodynamic Model

A Strathclyde internally developed code, HyFlow, is used instead of a more commonly used CFD tool. This aero-thermodynamic model is employed to evaluate the external heat flux and to estimate the value of the heat transfer coefficient. HyFlow is based on a combination of compression and expansion panel methods: it uses simplified equations and analogies to perform aero-thermal predictions of the heat flux values during hypersonic flight. The simulations are performed under the assumption of thermally and calorically perfect gas and the solver has the capability to generate estimations for both high altitude with free-molecular flow conditions and lower altitudes characterized by continuum flow. The heat flux is calculated by employing the flat plate reference temperature method for evaluating the skin friction. This method adopts an analogy based on the similarity between friction and heating mechanisms, called the Reynolds analogy[8]. A different methodology is implemented at the stagnation point for the reason that this analogy is not valid around this particular point. Instead, the Fay-Riddell [9] formula to calculate the convective heating rate for three-dimensional stagnation points is employed. This method evaluates the convective heating rate starting from the velocity gradients in both the streamwise and crosswise directions.

In the current development of the coupled approach the data that is communicated by the thermal response code to the aerodynamic solver is solely the surface recession values on the different vertices; thus only the changes in geometry during the trajectory influence the aerodynamic code. Other phenomena caused by the material ablation (e.g. blocking, pyrolysis gas flux) are not part of the shared data between codes therefore can not impact HyFlow simulations. These ablation effects do influence the aerodynamics but their influence is neglected in the current approach.

Code coupling

To perform the simulation, the trajectory of the spacecraft during the atmospheric crossing is divided into a number of points. For each of the points the external free stream velocity, pressure and temperature values are adopted by HyFlow as inputs to calculate the heat flux values for each panel of the capsule. The values of the heat flux on the vertices are computed by applying a simple interpolation from the panels values. Afterwards, the one dimensional material response code is applied on each vertex and it integrates for a duration equal to the difference between two consecutive trajectory points. For the first iteration between the two codes, all of the panels are considered to be composed of a fully virgin material at the same initial temperature. After the first iteration of the ablative code, the newly calculated values of temperature, changes in the material state and recession for every vertex are stored and used as initial conditions for the following iteration. The recession due to the pyrolysis is evaluated at the end of every material code integration and it is immediately applied on the capsule geometry in order to perform the simulation on the correct geometry for the entire trajectory duration. The ablative response code is applied on the vertices and not on the panels for the reason that the recession is easier applied on the vertices instead of the panels without introducing errors in the geome-

Table 1: Martian atmosphere properties used in HyFlow

γ	c_{pv}	R	P_r
1.33	730	192	1

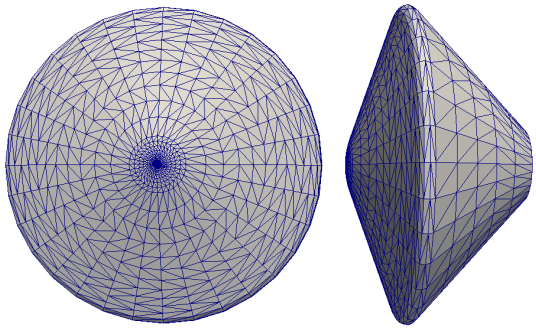

Fig. 1: Front and side representation of the Pathfinder geometry as it is utilised for the simulations in this paper.

try and because the number of vertices is inferior to the number of panels making the simulation faster.

Results

The Pathfinder probe performed a successful landing on Mars surface in 1997. The aerodynamic code applied in the approach herein presented has performed different Earth atmosphere simulations [1],[10] but this was the first Martian test case that the method has been applied to. Mars and Earth atmospheres differ greatly from one another, both in their composition and in their physical characteristics. HyFlow has the ability to simulate any atmosphere given the right properties, Table 1 summarizes the characteristics employed by the code to perform the simulation and the values that were selected to describe the Martian atmosphere. The capsule geometry is illustrated in Fig. 1, the forebody heat shield is formed by the SLA-561V material and has a thickness of 1.9 *cm*. The rest of the heat shield is composed of different materials and thickness; because studies for the leeward surfaced were not found in literature by the authors, it was decided to use the more simplified case and employ the same material with the same thickness for the entire geometry.

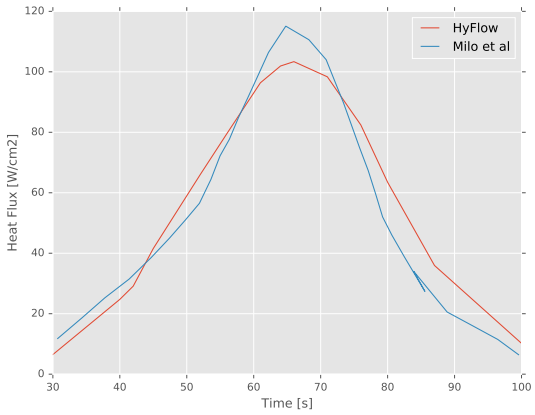

Fig. 2: Comparison of the heat flux as a function of time in the stagnatiuon point between the estimation presented by Milos et al [3] and the values calculated by the code heriein presented.

Nevertheless, the code herein utilized has the ability to handle different thickness and materials on different geometrical positions. The SLA-561V thermoablative model was created utilizing the data presented by Strauss [11]; unfortunately it is a single component model and it does not report in great precision the various thermal characteristics. The evaluations used to compare against were produced by Milos et al [3] using the GIANTS code, a CFD tool, for the external flux evaluations while the thermal response of the heat shield were produced using different models, in particular these were developed at Applied Research Associates (ARA), NASA Ames Research Center(ARC), and Lockheed Martin Astronautics(LMA). The CMA code was used for the ARA model, both FIAT and CMA were employed for the ARC model and REKAP code was used for the LMA model [3]. The first result shown in the present work is the heat flux as a function of time for the stagnation point, Fig. 2. The two curves are in good agreement even if the HyFlow heat flux peak is slightly inferior than the GIANT evaluated one; this small discrepancy was expected due to the use of a reduced order code for the environmental simulation in contrast with a CFD tool. Although some small differences are present the two trends are relatively close and the approximated heat flux can be used to generate the thermal simulations that can be used in preliminary design studies. If, for any reason, conservative results were to be preferred it is possible to multiply the evaluated heat flux by a desired coefficient. Fig. 3 illustrates the heat flux profile at the

Table 2: Time instances for the re-entry trajectory.

Time,s	Altitude,km	Velocity,m/s	Temperature,K	Density, kg/m^3
30	85.000	7504	105	6.74E-07
40	71.109	7496	122	7.24E-06
42	68.469	7490	129	1.01E-05
45	64.599	7472	112	2.10E-05
52	56.026	7364	143	5.76E-05
56	51.445	7242	157	9.28E-05
61	46.089	6994	162	1.69E-04
64	43.097	6774	168	2.31E-04
66	41.204	6596	169	2.80E-04
71	36.854	6041	173	4.38E-04
76	33.082	5333	170	6.68E-04
80	30.489	4717	175	8.53E-04
87	26.760	3704	179	1.24E-03
100	21.848	2299	184	2.01E-03

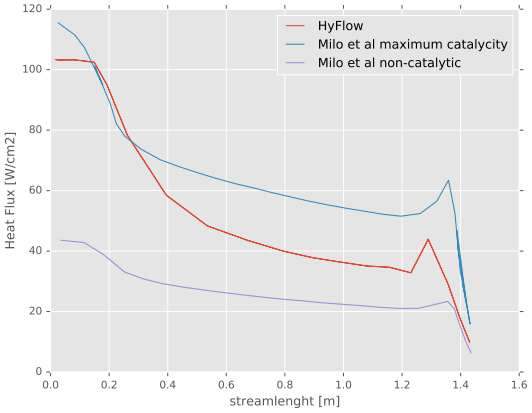

Fig. 3: Heat flux profiles along the capsule as presented in the papare by Milos et all [3] and as evaluated during this study for the time of peak heat flux.

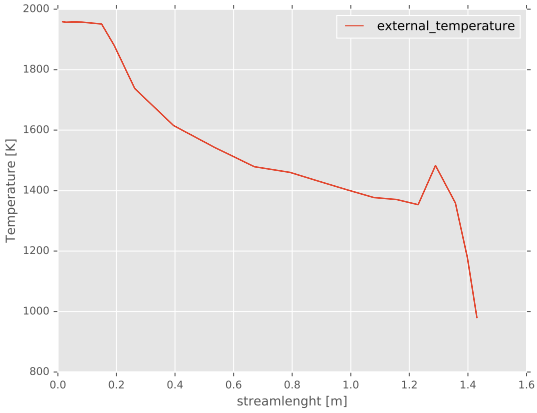

Fig. 4: Temperature profiles along the capsule as evaluated during this study for the time of maximum external temperature.

time of peak heat flux as evaluated by the current approach and as calculated by the reference paper for the case of maximum catalycity and the non catalytic case. The methodology used presents results inside these two extremes cases. The differences in the location of maximum value for the shoulder portion of the capsule can be attributed to the mesh; HyFlow is highly dependant on the mesh distribution and the mesh size, a more refined mesh could give closer results but it was decided not to increase the number of mesh panels for two main reasons. Firstly, because the authors were satisfied with the level of precision of the results and secondly, to avoid an increase in the simulation time since one of the aims of this study is to demonstrate that is is possible to produce reasonable evaluations of a three-dimensional atmospheric entry without significant computational effort. Fig. 4 shows the external temperature values on the capsule at the time of maximum temperature during the trajectory. The temperature and the heat flux have a very similar trend for the reason that the former is influenced by the latter. Lastly, the total recession of the capsule is shown in Fig. 5; as expected, this property presents a very similar trend to the temperature and the heat flux because it depends on both of those parameters. Three dimensional representations of the graphs shown in this section are

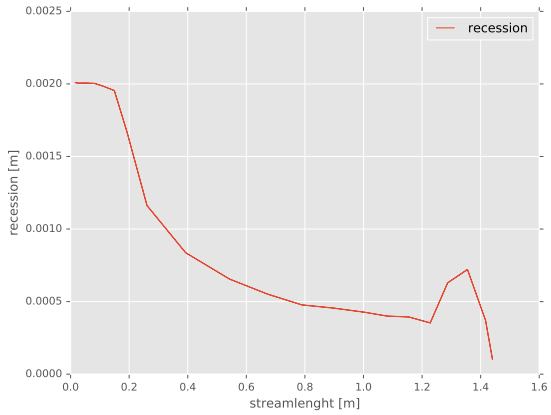

Fig. 5: Recession profiles along the capsule as evaluated during this study at the end of the simulation.

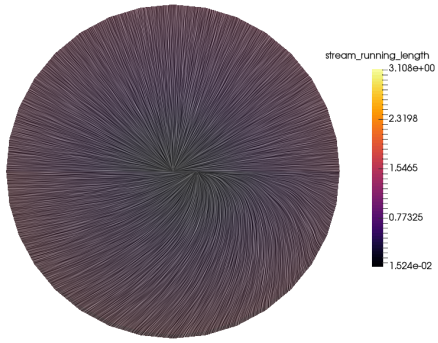

Fig. 6: Representation of the streamline. The upper half of the image represents the axi-symmetric case whlie the lower part illustrates the case with an angle of attack equal to 15 degrees.

present in the next section in comparison with a different test case. The test case herein presented is axi-symmetrical thus a simpler two dimensional evaluation can produce the same outcomes regarding the TPS behaviour as a three-dimensional one; nevertheless, real atmospheric entries are not perfectly axi-symmetric. To the authors knowledge, fully coupled three-dimensional simulations of the external environment and the thermo-ablative internal material behaviour are not currently available in the literature due to the computation time required. A non axi-symmetrical case can be simulated by the discussed approach with the same simplicity of an axi-symmetrical case. The following section illustrates the changes that the introduction of an angle of attack can produce in the heat flux and temperature trends and why it is important to be able to simulate it.

Non axi-symmetrical case

One of the features of the proposed approach is the ability to produce three dimensional approximated results. Unfortunately, to the authors knowledge, there are no three dimensional evaluations of the Pathfinder entry in literature. The results that have been used in the previous section to compare against were generated simulating in two dimensions an axi-symmetrical test case. However most capsules entering a planetary atmosphere do not have their axis of symmetry perfectly parallel to the velocity vector for the entire duration of the trajectory. The difference of angle in this case could lead to some serious consequences if the leeward surface, which is shadowed in the axi-symmetric case, is exposed to more elevated heat flux values than in the nominal case. To illustrate how small changes can influence the simulations, this section describes the results of a non axi-symmetric Pathfinder Martian entry and highlights the differences between this case and the one previously presented; to do so an angle of attack equal to 15 degrees was introduced. Fig. 6 shows the streamlines for the zero and non-zero angle of attack cases. Fig. 7 shows the comparison between the axi-symmetrical and the non axi-symmetrical case heat flux. It is highlighted how in the second case, the shoulder has a consistent increase of heat flux with respect to the nominal case. In the Pathfinder capsule, the shoulder is still adequately protected by the SLA-561V material of large enough thickness. Fig. 8 and Fig. 9 illustrate that both external temperature and surface recession present the same increase in the shoulder as the heat flux. The capsule in study has a back heatshield quite different from the forebody one. In particular, it has an ablative material used for lower heat fluxes and a heatshield thickness inferior with respect to the forebody one. If the heat flux values for this surface increase too much it is possible that the TPS will not be able to properly protect the spacecraft. This is the reason why it is important to perform simulations that are able to evaluate what happens when a small angle of attack is present during the entry trajectory. The case presented in this section is still symmetric and can be studied with a two dimensional geometry representing a full sec-

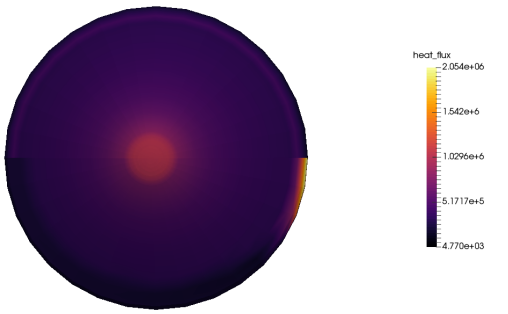

(a) The upper half of the image represents the axi-symmetric case whlie the lower part illustrates the case with an angle of attack equal to 15 degrees.

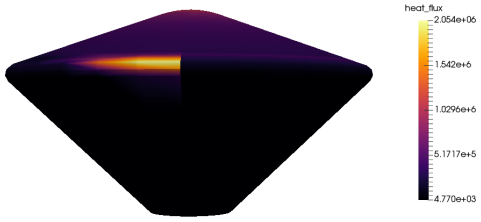

(b) The right part of the image represents the axi-symmetric case while the left side illustrates the case with an angle of attack equal to 15 degrees.

Fig. 7: Three dimensional representation of the heat flux at the time of peak heat flux for the geometry surface

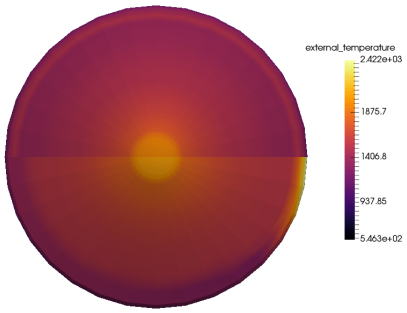

(a) The upper half of the image represents the axi-symmetric case while the lower part illustrates the case with an angle of attack equal to 15 degrees.

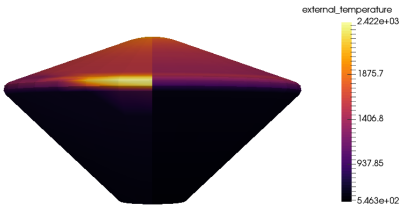

(b) The right part of the image represents the axi-symmetric case while the left side illustrates the case with an angle of attack equal to 15 degrees.

Fig. 8: Three dimensional representation of the external temperature at the time of maximum externa temperature for the geometry surface

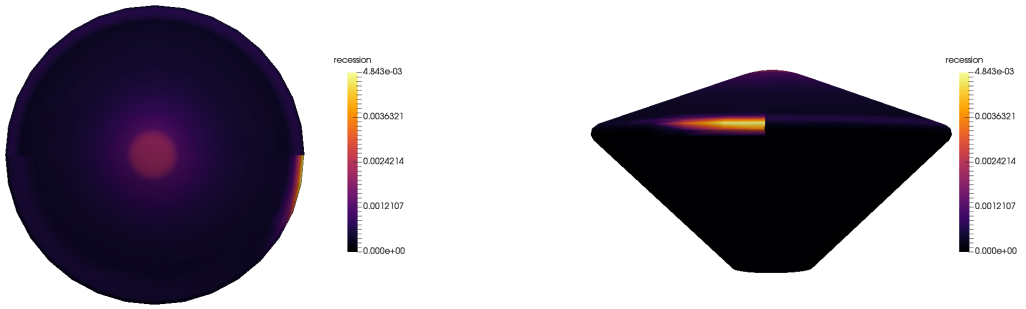

(a) The upper half of the image represents the axi-symmetric case while the lower part illustrates the case with an angle of attack equal to 15 degrees.

(b) The right part of the image represents the axi-symmetric case while the left side illustrates the case with an angle of attack equal to 15 degrees.

Fig. 9: Three dimensional representation of the suface recession at end of the trajectory for the geometry surface

tion of the capsule instead of half of the forebody section used in the axi-symmetric case. However this would highly increase the number of cells of the mesh, greatly increasing the computational time. The approach presented in this paper is to always perform three dimensional calculations of the atmospheric entry, therefore the symmetry of the flux or the lack of this symmetry does not influence the computational time. Consequently complex, non symmetric cases are just as easy to simulate as non symmetric ones.

Conclusions

The coupling of the material response code and the aero-thermodynamic model has been used to simulate a Martian atmosphere entry. The heat flux values along the trajectory have been evaluated and the ablative TPS behaviour has been computed. The comparisons presented in this paper show that the approach used produces results in good agreement with evaluations generated with more complex tools. The two coupled codes, which were already verified for Earth re-entry [10], are shown to be capable of performing simulations for the Martian atmosphere. Although the precision of the results is lower than the results produced with CFD tools or fully two dimensional ablative codes; nevertheless the evaluations are precise enough to give a good understanding of the external flux and internal material behaviour; especially in the preliminary phases of the mission design. Moreover, the simulations performed with this approach are not too computationally demanding; the simulation time depends on the number of trajectory points to evaluate, the total entry time and the mesh dimension. For the analyses herein presented the trajectory is divided into 14 points, its total duration is 70 s and the mesh is composed of 1242 vertices; the running time for a complete simulation is 22 minutes.

References

[1] Romain Wuilbercq. *Multi-Disciplinary Modelling of Future Space-Access Vehicles*. PhD thesis, Strathclyde University, 2015.

[2] David Olynick, Y.-K. Chen, and Michael E. Tauber. Aerothermodynamics of the Stardust Sample Return Capsule. *Journal of Spacecraft and Rockets*, 36(3):442–462, May 1999.

[3] Frank S. Milos, Y.-K. Chen, William M. Congdon, and Janine M. Thornton. Mars Pathfinder Entry Temperature Data, Aerothermal Heating, and Heatshield Material Response. *Journal of Spacecraft and Rockets*, 36(3):380–391, May 1999.

[4] Alexandre Martin and Iain D. Boyd. Strongly Coupled Computation of Material Response and Nonequilibrium Flow for Hypersonic Ablation. *Journal of Spacecraft and Rockets*, 52(1):89–104, January 2015.

[5] Carl B. Moyer and Mitchell R. Wool. Aerotherm Charring Material Thermal Response and Ablation Program, Version 3. Volume 1. Program Description and Sample Problems. Technical report, AEROTHERM CORP MOUNTAIN VIEW CA, 1970.

[6] Bernard Laub, Yih-Kanq Chen, and John Dec. Development of a High-Fidelity Thermal/Ablation Response Model for SLA-561v. American Institute of Aeronautics and Astronautics, June 2009.

[7] Y.-K. Chen and F. S. Milos. Two-Dimensional Implicit Thermal Response and Ablation Program for Charring Materials. *Journal of Spacecraft and Rockets*, 38(4):473–481, July 2001.

[8] W. L. Hankey. Re-entry aerodynamics. *American Instituteof Aeronautics and Astronautics,*, Washington, DC, 1988.

[9] H. H. et al Hamilton. Approximate Method of Calculating Heating Rates at General Three-Dimensional Stagnation Points During Atmospheric Entry. 1982.

[10] V. Renato, T. Scanlon, and R. Brown. Multi-dimensional ablation and thermal response program for re-entry analysis. *31st International Symposium on Space Technology and Science*, 2017.

[11] S. D. Williams and Donald M. Curry. Thermal protection materials: thermophysical property data. 1992.